# BEAM SWEEPING SYSTEM

F.M. Bieniosek[+], O. Kurnaev†, A. Cherepakhin†, J. Bielicki
*Fermi National Accelerator Laboratory[*], Batavia, IL 60510*

J. Dinkel
*Creative Designs, Inc., Oak Brook, IL 60523*

*Abstract*

The sweeping system deflects high-energy proton and antiproton beams in a single-turn rotating-field magnet that combines deflection in both planes into a single unit. The magnet current has a peak amplitude of 10 kA and the sweep time is 1.6 µs. At the Fermilab Antiproton Source increasing proton beam intensities incident on the antiproton production target threaten to damage the target. The purpose of the sweep magnet is to spread the hot spot on the target with a sweep radius of up to 0.5 mm, greatly reducing the peak energy deposition.

## 1 INTRODUCTION

At Fermilab, antiprotons are collected from the interaction of a 120-GeV proton beam with a solid nickel target. The efficiency of collecting antiprotons from the target rises as the size of the proton beam spot on the target is reduced. However at the same time the peak energy deposition on target rises. Under Main Injector conditions (5 x $10^{12}$ protons in a 1.6-µs pulse with a repetition rate of 1.5 seconds), the spot size will have to be increased to at least 0.25 mm to keep peak energy deposition near current levels. To bring the density of energy deposition with a 0.1-mm spot size down to currently-existing levels, a system to sweep the beam spot on the target [1] has been under development. Larger sweep radii will be required if proposed upgrades for the Main Injector [2], e.g., "slip stacking", result in increases in proton intensity.

Figure 1 shows a layout of the target station. Two upstream sweep magnets will be installed at the end of the 120-GeV proton beamline (after quadrupole magnet PQ9B). This location is the focal point of the proton lithium lens[3]. Antiprotons created in the target are collected by a lithium lens, and deflected by the pulsed magnet into the AP2 beam line for collection in the Debuncher. A single downstream sweep magnet will redirect the 8 GeV antiprotons parallel to the AP2 beamline.

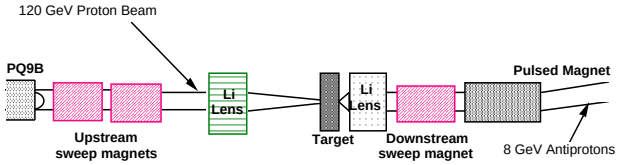


Figure 1. Major components in the target station. The three sweep magnets are identical.

## 2 SWEEP MAGNET

The beam sweeping system traces a 0.33 to 0.5-mm-radius circular pattern on the target over the 1.6-µs proton beam pulse. The magnets have a 2-phase, 4-conductor winding excited by two power supplies that deliver balanced 625 kHz sinusoidal current waveforms in quadrature to generate a 625-kHz rotating dipole field[1]. The magnetic field due to two pairs of current-carrying conductors oriented 90¤ apart is rotating on axis if the current in the two pairs of conductors is $I_0\cos(\omega t)$ and $I_0\sin(\omega t)$. If the conductors are twisted such that the axial current integrated over the length of the magnet has the distribution $I_0\sin(\omega t-\theta)$, the line integral of the field along the beam path is uniform and rotating.

The average deflecting field required for a 0.5-mm sweep radius is 1.26 kG on the downstream sweep magnet, which is 56 cm long. Because of the twist in the conductors, the peak field on axis must be a factor $4/\pi$ times larger than the average field, or 1.60 kG. The ratio of the magnet current to the local magnetic field on axis, calculated by POISSON for a straight conductor, is 6.1 A/Gauss. Thus to provide the desired field, the peak current required from the power supply is 9.8 kA, and the peak inductive voltage drop across the magnet is 7.7 kV (peak voltage to ground 3.85 kV) for a magnet inductance of 0.2 µH.

A cross sectional view of the sweep magnet is shown in Figure 2. The clear bore of the magnet is 28.5 mm. The region of antiproton flux that is collected downstream has a diameter of 22 mm. The conductors are hollow 6.35-mm diameter aluminum tubes. Hollow aluminum tubes were chosen to minimize the beam-induced heating of the conductors, and to allow the passage of cooling air through the center of the conductors. A ceramic tube provides electrical insulation between the conductor assembly and the magnetic cores. No vacuum wall is required, because the beam is transported through air

---

[*]Operated by the Universities Research Association Inc., under contract with the U.S. Department of Energy.

[+]Present address: LBNL, Berkeley, CA 94720, email fmbieniosek@lbl.gov

†On leave IHEP, Protvino, Russia

from upstream of the target to downstream of the pulsed magnet. Molybdenum Permalloy Powder (MPP) cores were chosen for the magnet yoke. The core material has relatively low losses, and adequate inorganic insulation. A magnet assembled with powder cores has the advantages of ease of construction, and the relatively high thermal conductivity and Curie temperature of this material. The fairly small thermal stresses are contained by press-fitting the cores in a water-cooled nickel housing. Estimated beam thermal power is 54 Watts per core at 1 x $10^{13}$ protons per pulse, or a total power of 1944 Watts for all 36 cores.

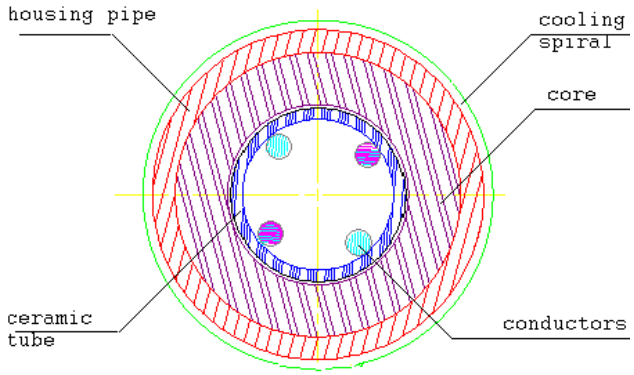


Figure 2. Sweep magnet cross section.

A longitudinal view of the magnet is shown in Figure 3. The current leads are located in the midplane of the magnet. The conductors are grounded at the end ring by the end flange on both sides of the magnet. Four ceramic bushings are used to support the current leads and insulate them from the magnet body. Silver-coated beryllium copper finger stock is attached between thin copper rings and copper spacers. The copper spacers are located between each two pairs of cores. The fingerstock serves as a slide guide and stress relief for the insulating ceramic tube, and provides a thermal conductive path for removal of beam-induced heating from the tube and current conductors.

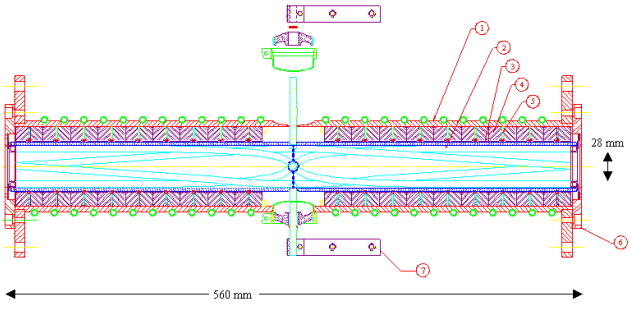


Figure 3. Longitudinal cross section of rotating field magnet. 1 - housing pipe, 2 - twisted conductors, 3 - ceramic pipe, 4 - MPP core, 5 - spacer, 6 - end flange, 7 - current lead

Magnetic measurements of the sweep magnet were performed with stretched wires. Ribbon cable was used to pick up the dB/dt signal along the whole magnet length and then was integrated to obtain a signal proportional to magnetic flux through the measurement loop. The signal amplitude was as expected. The line-integrated field distribution was uniform within ±1% over a 20-mm horizontal window for three planes at 0 and ±7mm vertical offset from center.

## 3 POWER SUPPLY

Power will be supplied through coaxial cables over a distance of approximately 10 m into the target vault, and (for downstream magnet) by 2.5 m of strip line through steel shield modules to the magnets at the bottom of the target vault. A simplified circuit diagram is depicted in Figure 4. The solid-state power supply is based on a two-stage compression circuit with saturating reactors. Pulse compression facilitates transfer of the current pulse to the ringing circuit in a high-radiation environment. An SCR switch is used for resonant charging of the first stage capacitor C1 using the leakage reactance of a 1:10 step-up transformer.

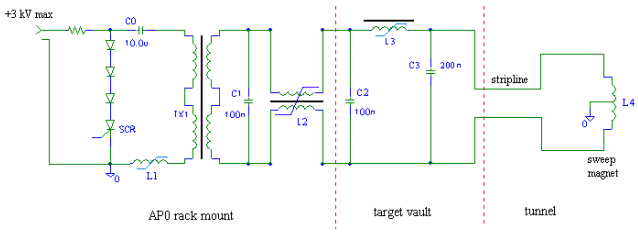


Figure 4. Simplified schematic diagram of power supply.

Energy storage capacitor C0 is initially charged up to 3 kV by the DC high voltage supply. The energy is transferred to the first compression stage capacitor C1 via the step-up transformer by closing the thyristor switch SCR. The small saturating choke $L_1$ protects the SCR by limiting the initial dI/dt of the thyristor switch to 100 A/μs for the first microsecond after turnon. To limit the reverse current of the thyristor, which has a relatively long recovery time, a stack of fast recovery diodes is connected in series. When the first saturating reactor L2 becomes conductive the energy from C1 transfers to the second stage capacitor C2. The second stage is located about 10 m away in a high radiation area and is connected to the first stage by a pair of coaxial cables (RG 220/U). Saturation of L3 initiates the discharge of C2 into the ringing circuit L4, C3. Capacitor C3 is connected to the sweep magnet (inductance L4) via the strip line.

The first stage switching reactor L2 is wound on four 2.3 mV-sec/turn Magnetic Metals Square-50 (25 μm) nickel-iron tape cores. The winding is split into two equal halves. Each half has 8 turns. The circuit between the step-up transformer and the reactor is balanced, with peak voltages of ±15 kV. When the reactor saturates, the voltages on the two terminals of C1 approach 15 kV, and

the voltage on one of the two output terminals approaches 30 kV. The other terminal remains at ground potential until the second reactor saturates. A DC bias current of up to 5 A is provided for both reactors L2 and L3.

The second stage reactor is wound on three 3.0 mV-sec/turn Allied-Signal 2605-SC Metglas cores, annealed and cowound with 3-µm mylar insulation. The reactor L3 has 4 turns. With these windings, the volt-seconds capability of the cores is 150 mV-sec for the first stage, and 36 mV-sec for the second stage. Inductive voltage per lamination in the first stage is about 0.6 V, and in the second stage about 2.2 V. Nickel-iron tape cores were chosen for the first stage because of their very square B-H loop, relatively large packing factor, acceptable losses and adequate insulation. Metglas cores were chosen for the second stage because of their small losses and good insulation properties of the mylar film.

Measurements of the losses in energy transfer were made at 2.9 kV. The initial energy stored on capacitor C0 was 42 J. Energy delivered to capacitor C1 was 35 J. Of the 7 J loss in this energy transfer the losses were distributed 4 J to the SCR switch and 3 J to the balance of the circuit. Energy transferred from C1 to C2 was 31.5 J. The losses were dominated by resistive losses in the windings. Switching losses in the cores, determined from the B-H loops, are small, 0.3 J in the first stage, and 0.5 J in the second stage. Energy transferred to the ringing circuit was 22 J.

The least efficient part of the circuit is the final transfer from capacitor C2 to the ringing circuit L4, C3. When the reactor L3 saturates, a single current pulse passes to the ringing circuit. It is relatively inefficient for two reasons.

First, it is necessary to prevent saturating the reactor a second time, and passing a second reverse current pulse that effectively extracts energy from the magnet circuit. The necssary voltage reversal is naturally accomplished if the ratio of capacitor C3 to capacitor C2 is at least 2. This reflected voltage also provides a reset pulse to the reactors, ensuring highly stable operation even with no reverse bias current.

Second, some current flows in the inductance of the sweep magnet, L4, before the energy transfer is completed. For typical saturated inductance of the output switch, about 0.5 µH, the efficiency of final energy transfer is about 80%.

The power supply was built and tested for 7 million pulses at 3 kV (full charge). At 3 kV charge, the output current amplitude is 11.6 kA. Oscilloscope pictures of voltages and currents under typical operation are shown in Figures 5 and 6. Power supply jitter does not exceed ±2 ns, while slow drift is about 20 ns. Installation of the complete system is expected in the year 2000.

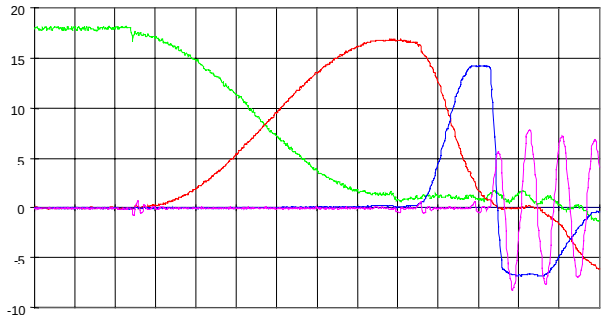


Figure 5. Scope picture of voltages in compression stages. Initial voltage = 1.8 kV. Vertical scale = 5 kV/div, horizontal scale = 2 µs/div. Green - first charging capacitor x 10. Red - first compression stage capacitor. Blue – second compression stage capacitor. Pink - ringing circuit (magnet) voltage.

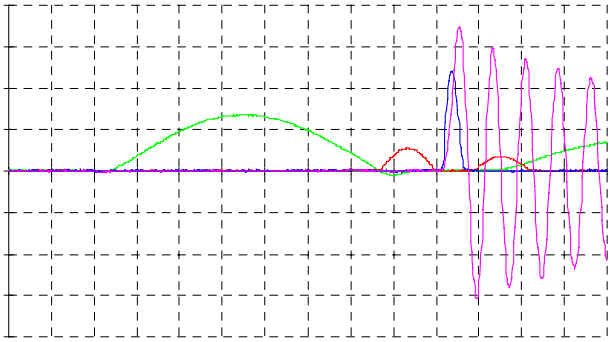

Figure 6. Scope picture of currents in compression stages of power supply. Peak magnet current is 7 kA, corresponding to 2.2 kV charge. Vertical scale = 2 kA/div, horizontal scale = 2 µs/div. Green - SCR current. Red - first compression stage. Blue - second compression stage. Pink - ringing circuit (magnet) current.

## 5 REFERENCES

[1]. F. M. Bieniosek, O. Kurnaev, A. Cherepakhin, J. Dinkel, Proc. 1997 Particle Accelerator Conference, paper 8P10.

[2] P.P. Bagley, et. al., Summary of the TeV33 Working Group ,in *1996 Snowmass Conf.*

[3] F. M. Bieniosek and K. Anderson, Lithium Lens for Focusing Protons on Target in the Fermilab Antiproton Source, Proc. Particle Accelerator Conf, Washington, 1993.